Effect of Subcooling on Pool Boiling of Water from Sintered Copper Microporous Coating at Different Orientations

UT Dallas Author(s):

Seongchul Jun
Jinsub Kim
Seung M. You

Citation:

Jun, S., J. Kim, S. M. You, and H. Y. Kim. 2018. "Effect of subcooling on pool boiling of water from sintered copper microporous coating at different orientations." Science and Technology of Nuclear Installations 2018: art. 8623985, doi:10.1155/2018/8623985

Hindawi
Science and Technology of Nuclear Installations
Volume 2018, Article ID 8623985, 9 pages
https://doi.org/10.1155/2018/8623985

Research Article

Effect of Subcooling on Pool Boiling of Water from Sintered Copper Microporous Coating at Different Orientations

Seongchul Jun,[1] **Jinsub Kim**,[1] **Seung M. You**,[1] **and Hwan Yeol Kim**[2]

[1]*Department of Mechanical Engineering, The University of Texas at Dallas, 800 W. Campbell Rd. Richardson, TX 75080, USA*
[2]*Korea Atomic Energy Research Institute (KAERI), Severe Accident & PHWR Safety Division, 989-111 Daedeok-Daero, Yuseong-Gu, Daejeon, Republic of Korea*

Correspondence should be addressed to Seongchul Jun; seongchj@gmail.com

Received 22 March 2018; Revised 29 June 2018; Accepted 22 July 2018; Published 13 August 2018

Academic Editor: Iztok Tiselj

The subcooling effect on pool boiling heat transfer using a copper microporous coating was experimentally studied in water for subcoolings of 10 K, 20 K, and 30 K at atmospheric pressure and compared to that of a plain copper surface. A high-temperature thermally conductive microporous coating (HTCMC) was made by sintering copper powder with an average particle size of 67 μm onto a 1 cm × 1 cm plain copper surface with a coating thickness of ~300 μm. The HTCMC surface showed a two times higher critical heat flux (CHF), ~2,000 kW/m^2, and up to seven times higher nucleate boiling heat transfer (NBHT) coefficient, ~350 kW/m^{2}K, when compared with a plain copper surface at saturation. The results of the subcooling effect on pool boiling showed that the NBHT of both the HTCMC and the plain copper surface did not change much with subcooling. On the other hand, the CHF increased linearly with the degree of subcooling for both the HTCMC and the plain copper surface. The increase in the CHF was measured to be ~60 kW/m^2 for every degree of subcooling for both the HTCMC and the plain surface, so that the difference of the CHF between the HTCMC and the plain copper surface was maintained at ~1,000 kW/m^2 throughout the tested subcooling range. The CHFs for the HTCMC and the plain copper surface at 30 K subcooling were 3,820 kW/m^2 and 2,820 kW/m^2, respectively. The experimental results were compared with existing CHF correlations and appeared to match well with Zuber's formula for the plain surface. The combined effect of subcooling and orientation of the HTCMC on pool boiling heat transfer was studied as well.

1. Introduction

Subcooled boiling is an effective heat transfer mode that utilizes both single-phase and two-phase heat transfer for the cooling of high heat flux devices. One example is the cooling of an external reactor vessel wall by subcooled water when a severe accident occurs at a nuclear power plant from a natural disaster or malfunction. To protect the reactor vessel, the external reactor vessel wall must be cooled by a coolant. Heat transferred to the coolant must be maintained below the critical heat flux (CHF), which is the maximum heat flux before transitioning to the film boiling heat transfer. Others applications include high heat flux electronic chip cooling for electronic devices.

Many researchers have investigated the subcooling effect on boiling heat transfer, and some correlations have been developed for the subcooling effect on the CHF. Kutateladze [1] was one of the earliest researchers who investigated the subcooling effect. He postulated that the CHF was reached when vapor film being generated between the heater wall and the liquid as well as the increase in the CHF at the subcooling was due to the necessity of supplying an additional amount of heat to warm the subcooled liquid around a heated surface to saturation. Then, he formulated a CHF correlation between subcooling ($q''_{CHF,sub}$) and saturation ($q''_{CHF,sat}$), starting from heat balance and dimensional analysis as

$$\frac{q''_{CHF,sub}}{q''_{CHF,sat}} = 1 + C\left(\frac{\rho_l}{\rho_v}\right)^n \frac{c_{pl}}{L_{lv}}\left(T_{sat} - T_l\right) \quad (1)$$

where C is an empirical constant, ρ_l and ρ_v are liquid and vapor density, respectively, c_{pl} is the specific heat of liquid, L_{lv} is the latent heat of vaporization, and (T_{sat}-T_l) is the temperature difference between saturation (T_{sat}) and

bulk liquid temperature (T_l). The properties are based on the saturation temperatures. Next, he obtained the constant C=0.065 and n=0.8 in (1) from the experimental results of Kutateladze and Schneiderman [2] for water (1–3 atm), alcohol (1–10 atm), and isooctane (1 atm).

Ivey and Morris [3] created a correlation based on the vapor-liquid exchange mechanism developed by Engelburg-Forster and Grief [4] and Kutateladze's CHF formula (see (1)) and found the constant C=0.1 and n=0.75 in (1) by matching the experimental results of Kutateladze and Schneiderman [2]. Ivey and Morris [5] further investigated the effects of subcooling on stainless steel and Zircaloy-2 with a different diameter and wall thickness of test heaters by experiment. From their experimental results, they concluded that the CHF of subcooled boiling has a negligible difference for heater diameter and thicknesses as well as the materials for subcooling of 10–70 K.

Zuber et al. [6] developed a CHF correlation for subcooling without curve fitting with experimental results, but by postulating that additional heat flux is transferred to the subcooled liquid in addition to the same hydrodynamic crisis at saturation. The additional heat flux for the subcooled liquid to heat up to the saturation was expressed as a one-dimensional diffusion equation:

$$q'' = \frac{2k_l\left(T_{sat} - T_l\right)}{\sqrt{\pi\alpha\tau}} \tag{2}$$

where α is the thermal diffusivity and τ is the residence time that represents bubble cycle time.

The CHF for subcooled conditions is then expressed as

$$q''_{CHF,sub} = 0.131 L_{lv}\rho_v\left[\frac{\sigma g\left(\rho_l - \rho_v\right)}{{\rho_v}^2}\right]^{1/4} + \frac{2k_l\left(T_{sat} - T_l\right)}{\sqrt{\pi\alpha\tau}} \tag{3}$$

The first term on the right hand side of (3) is the CHF at saturation, and the second term is the additional heat flux caused by subcooling. After rearranging (3) and finding τ, it can be written as the form of CHF ratio between saturation and subcooling:

$$\frac{q''_{CHF,sub}}{q''_{CHF,sat}} = 1 + 5.32\frac{\left(k_l\rho_l c_{pl}\right)^{1/2}}{\rho_v L_{lv}}\left[\frac{\rho_v^2 g\left(\rho_l - \rho_v\right)}{\sigma^3}\right]^{1/8}\left(T_{sat} - T_l\right) \tag{4}$$

where k_l is the thermal conductivity of the liquid, g is the gravitational acceleration, and σ is the surface tension. It can be seen from (4) that the CHF increases proportionally with subcooling. This correlation showed good agreement with the experimental results done by Kutateladze and Schneiderman [2] for water and ethyl alcohol. Many other correlations of the CHF between subcooling and saturation have been developed so far, but the aforementioned three correlations are the most well-known ones, especially for water, and the current experimental results are compared with them and discussed in Section 3.

Later subcooling effects on pool boiling heat transfer of dielectric liquids were studied as a cooling method for electronics as well [7–9]. Hwang and Moran [7] conducted a subcooling experiment of FC-86 on a vertical 4.57 mm square silicon chip in the range of 2–82 K and compared it with Ivey and Morris's [3] correlation to find that the value of the constant in the correlation was C=0.05 and n=0.75, which was half of the original Ivey and Morris correlation [3]. Mudawar and Anderson [8] studied the subcooling effects of FC-72 with a subcooling of 0–35 K on a vertical 12.7 mm × 12.7 mm flat surface and found the coefficient to be C=0.064 and n=0.75. Watwe et al. [9] investigated the subcooling effects of FC-72 on a horizontal 10 mm × 10 mm silicon chip and found the constant to be C=0.03 and n=0.75 by curve fitting with their experimental data. Those subcooling data of dielectric liquids showed lower coefficients (C=0.03–0.065) compared to water, which was 0.1 in the Ivey and Morris correlation [3].

Rainey et al. [10, 11] investigated the subcooling effects of a plain 10 mm × 10 mm flat copper surface in FC-72 and compared them with an ABM (aluminum particles, Devcon Brushable Ceramic epoxy, and methyl ethyl ketone) coating with a coating thickness of ~50 μm at a subcooling temperature of 0–50 K. They found that nucleate boiling heat transfer was closely maintained regardless of subcooling. They observed that the CHF of the ABM coating increased at a higher rate than that of the plain copper surface as the subcooling increased. Parker and El-Genk [12] investigated the subcooling effects of a plain 10 mm × 10 mm flat copper block and compared them with a porous graphite surface in FC-72 and reported that the CHF ratio between the porous graphite and the plain surface increased from 1.6 at saturation to 2.1 at 30 K of subcooling. El-Genk and Suszko [13] studied the effect of subcooling in PF-5060 on a dimpled surface and a plain surface and reported the rate of increase in CHF for the dimpled surface being 20% less than that of plain copper.

So far, many researchers have investigated the effects of enhanced surfaces on subcooled boiling with various fluids, but there have been few attempts to systematically investigate the effects of subcooling on pool boiling from enhanced surfaces for water. In the present study, the subcooling effect of copper microporous coatings created by sintering, called high-temperature thermally conductive microporous coatings (HTCMCs), was experimentally investigated with subcooled water of 10–30 K and compared with the results of a plain surface. Then, the experimental results of both the HTCMC and the plain surfaces were compared with the aforementioned correlations [1, 3, 6]. Finally, the combined effects of subcooling and orientation on the boiling heat transfer of the HTCMC at 30 K subcooling were investigated and compared with the previous study of orientation effects at saturation.

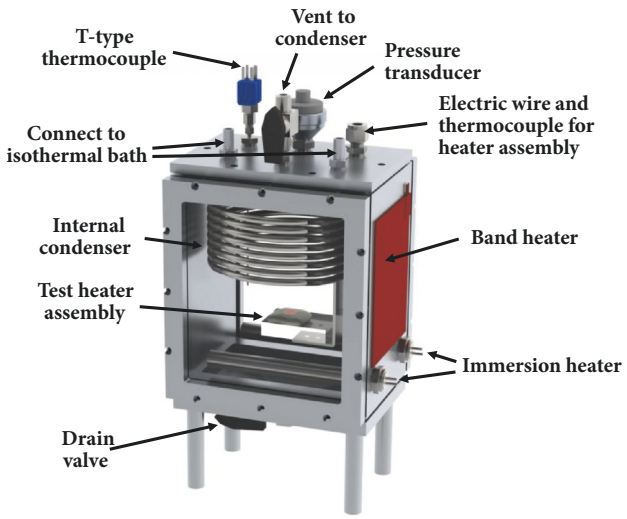

Figure 1: Schematic of the pool boiling chamber.

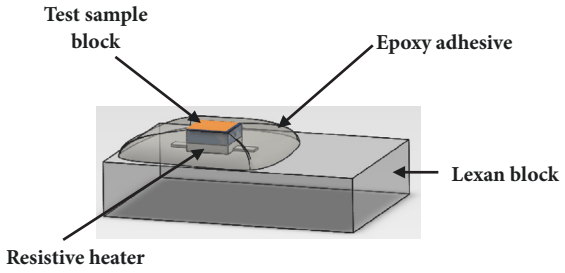

Figure 2: Schematic of test heater assembly.

2. Pool Boiling Experiments

2.1. Experiment Setup and Test Procedure. An aluminum chamber was used, as shown in Figure 1. It includes T-type thermocouples, a pressure transducer, internal and external condensers, band and immersion heaters, and a test heater assembly. The T-type thermocouples measured the bulk liquid temperature and the heater temperature. The pressure transducer measured the system pressure. Band and immersion heaters were attached to heat the liquid to the desired subcooling temperature and maintain the temperature during the pool boiling experiment. The stainless steel internal condenser was installed in the chamber and connected to an isothermal bath (Fisher Scientific, ISOTEMP 4100R28 Refrigerated/Heated Bath Circulators) in order to keep the bulk liquid at a constant subcooling temperature during the pool boiling tests. The test heater assembly was located on an aluminum bracket in the chamber and connected to electric wires and a T-type thermocouple.

The detailed configuration of the test heater assembly is shown in Figure 2. A test sample copper block (10 mm × 10 mm × 3 mm, k = 401 W/mK), which includes the sintered HTCMC on the top, was soldered to a resistive heater. The test sample block and the resistive heater pair were bonded to a 1.27 cm thick Lexan block (k = 0.2 W/mK) with a 3 M epoxy adhesive. The sides of the pair were insulated using the 3 M epoxy as well. Two electrical wires were soldered on each side of the bus bar to supply electrical power to the resistive heater, and a T-type thermocouple wire was inserted in the center of the copper block from the side. The top surface temperature of the test sample block below the HTCMC was calculated by assuming one-dimensional heat conduction through the copper block from the temperature measured by the thermocouple.

The pool boiling chamber was filled with distilled water and heated to the desired subcooled temperature at atmospheric pressure using the band and immersion heaters. Once the water reached the desired subcooled temperature, the liquid was maintained at a nearly constant temperature with little temperature fluctuation (< ±0.5 K) throughout a pool boiling test by controlling the temperature of the cooling water running through the internal condenser supplied from the isothermal bath and the band heaters operated with a temperature controller. All subcooled pool boiling experiments were conducted using the test heater assembly at various subcooled temperatures from 10 to 30 K under increasing heat flux conditions until the CHF condition was reached. During the experiment, the heat fluxes were supplied from a DC power supply (Agilent Technologies, N5771A) to the resistive heater of the heater assembly and measured by a data acquisition system (Agilent Technologies, 34980A Multifunction Switch/Measure Unit) controlled by the LabVIEW program installed on a PC. The heat fluxes were increased to the next value of the heat flux by a programmed value after they assumed a steady state if the differences between two consecutive averages of 40 data for 20 seconds each were less than 0.1 K. The CHF was declared once the instantaneous temperature jump was larger than 20 K compared to the immediately before averaged value, and the DC power supply was stopped by the program automatically. The CHF was defined as the heat flux of the last steady state plus half of the heat flux increment that was 25 kW/m^2.

2.2. Cu-HTCMC Fabrication. In order to create the Cu-HTCMC, copper powder (Alfa Aesar, 99.5%) with an average particle size of 67 μm was used. The particle size was measured using an optical microscope, and the particle distribution is shown in Figure 3. The copper powder was mixed with a specially made thinner and spread over a 1 cm × 1 cm copper block and dried. Then, the sample was sintered in a furnace at high vacuum (~10^{-5} hPa). After sintering, the sample was cleaned with 5% acetic acid by sonication and rinsed with distilled water.

The SEM image in Figure 4 shows that the HTCMC has porous structures, with a porosity (ε) of 0.65±0.03 found by calculating the measured volume of the porous layer (V_t) and the weight of the copper powders (m_{cp}):

$$\varepsilon = \frac{V_t - \left(m_{cp}/\rho_{cp}\right)}{V_t} \tag{5}$$

where ρ_{cp} is the density of the copper powders (8.96 g/cm^3).

2.3. Uncertainty Analysis. The experimental uncertainties for the current study were estimated by single-sample

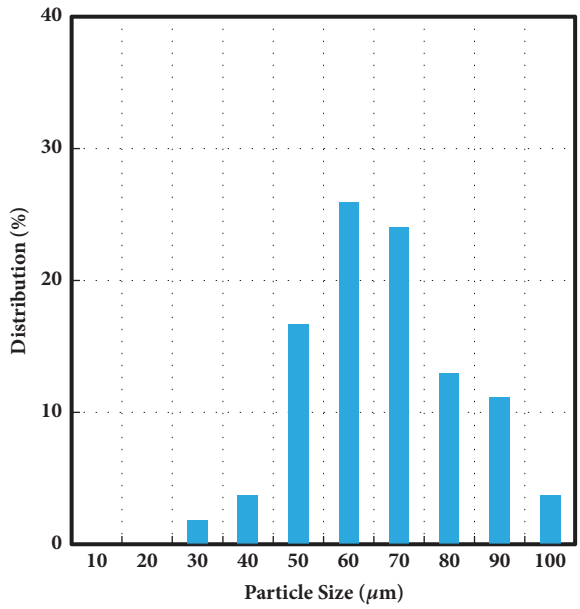

Figure 3: Particle size distribution with an average size of 67 μm. The sizes were measured using optical microscope images of Cu powders.

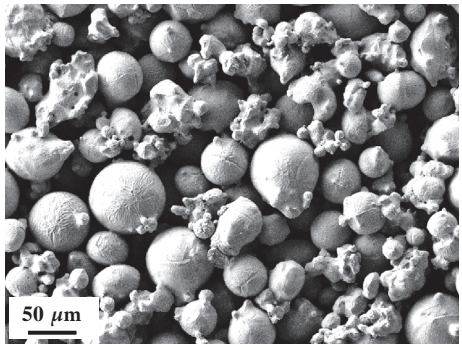

Figure 4: SEM of HTCMC sintered copper particles.

uncertainties using the method which was developed by Kline and McClintock [14]. Heat flux measurement uncertainty caused by the current, voltage, and surface area of the heater was estimated to be less than 5% with a 95% confidence level. From numerical simulation, the heat loss through the Lexan and epoxy insulation of the heater was estimated to be less than 0.5%. The temperature accuracy combined from the T-type thermocouple and the data acquisition system was estimated to be ±0.5 K.

3. Results and Discussion

The pool boiling of the subcooled water was studied experimentally for subcoolings of 10, 20, and 30 K at atmospheric pressure for both the plain copper and HTCMC surfaces. The plain copper surface was polished with a 600 grit sand paper. For the HTCMC, a copper powder with an average particle size of 67 μm with ~300 μm coating thickness was tested, which appeared to be the most enhanced nucleate

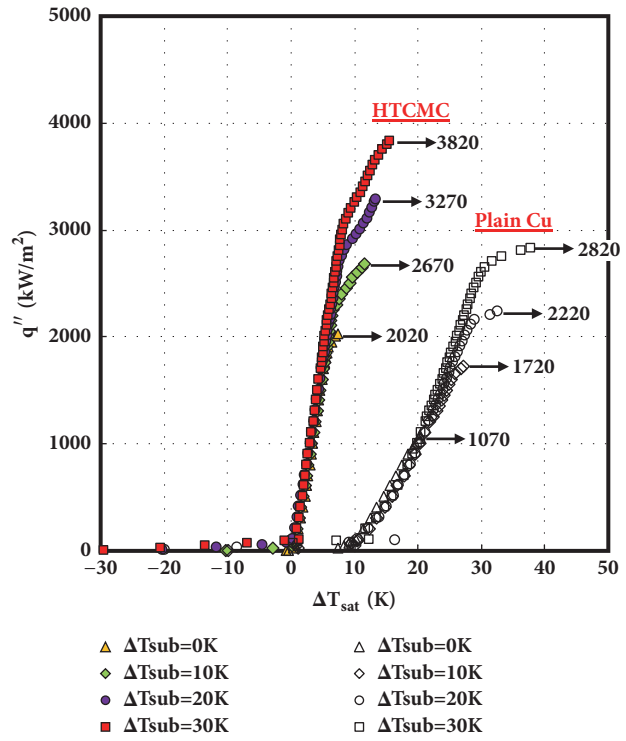

Figure 5: Boiling curves of HTCMC and a plain Cu surface at subcoolings.

boiling heat transfer (NBHT) and critical heat flux (CHF) [15]. The results at saturation showed that the NBHT and the CHF (the numeric values next to the arrows in Figure 5) are significantly enhanced compared to those of a plain surface, as shown in Figure 5. According to Jun et al. [16], the enhancement of the NBHT coefficient of the HTCMC is attributed to its porous structure with micron-scale cavities and reentrant-type cavities which create larger embryonic bubbles. Reentrant-type cavities are stable in generating vapor bubbles even at low wall superheat by combining the effects of their geometry and the thermodynamic aspects of the fluid [17]. The condition for an embryonic bubble growing in a cavity can be expressed by combining the Young–Laplace and Clausius–Clapeyron equations [18]:

$$\Delta T_{sat} \cong \frac{2\sigma T_l v_{lv}}{L_{lv} R_c} \quad (6)$$

where ΔT_{sat} is the wall superheat ($=T_s - T_{sat}$), σ is the surface tension of bulk liquid at saturation, T_l is the bulk liquid temperature, v_{lv} is the specific volume difference between vapor and liquid ($=v_v - v_l$), L_{lv} is the latent heat of vaporization, and R_c is the radius of liquid/vapor interface curvature in a cavity. According to (4), a smaller wall superheat (ΔT_{sat}) is required at larger R_c to make the embryonic bubble grow. Reentrant-type cavities in the HTCMC have a significantly larger R_c compared to those of the plain copper surface, so the wall superheat needed for the embryonic bubble to grow in the HTCMC must be much smaller. Therefore, it leads to the increased number of nucleation sites and NBHT enhancement of the HTCMC.

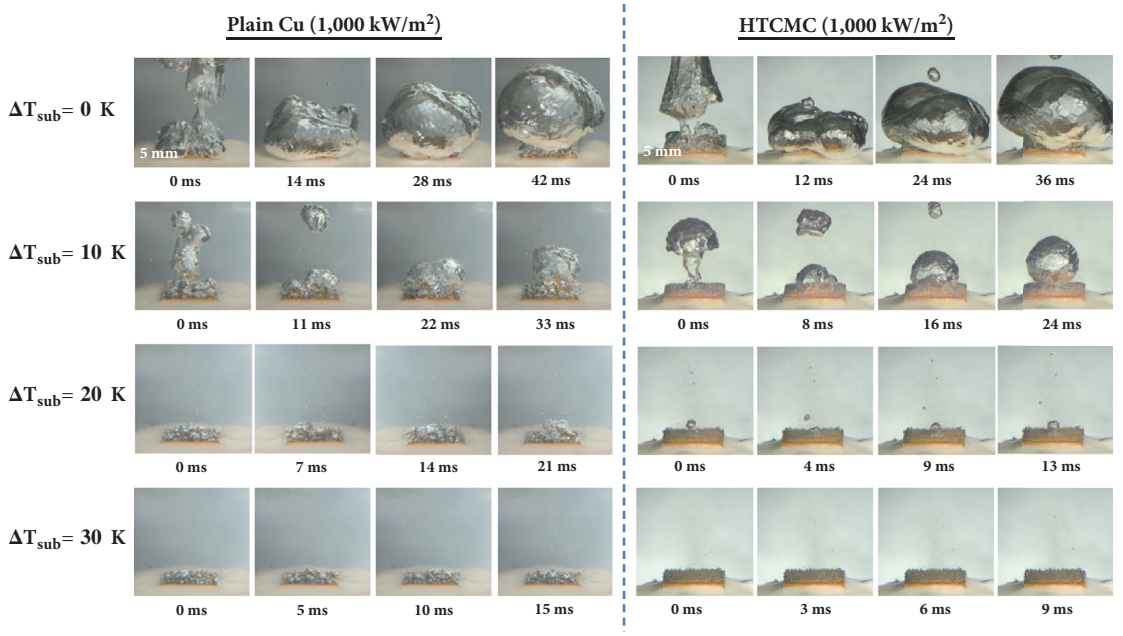

Figure 6: Nucleate boiling comparison of Plain Cu and HTCMC with different subcooled temperatures (ΔT_{sub}) of 0 K, 10 K, 20 K, and 30 K at a heat flux of 1,000 kW/m^2.

The subcooled pool boiling of both the HTCMC and the plain copper surfaces revealed that the wall superheats at different subcoolings were close at heat fluxes up to ~ 2,000 kW/m^2 and ~1,000 kW/m^2, each being near the CHF at saturation. This insensitivity effect of subcooling on NBHT is consistent with previous literature [4, 10–12, 17, 19, 20]. According to Engelburg-Forster and Grief [4], the combined effects of smaller bubble departure diameter and shorter bubble cycle at subcooling make the NBHT little difference at the same heat fluxes. The same trend was observed from the current study. Therefore, the enhancement of the NBHT in the HTCMC was maintained throughout the subcoolings. In other words, the wall superheats of the HTCMC for all the subcooled boiling remained below 5 K for the heat flux of 1,500 kW/m^2, and this is the significant enhancement of the nucleate boiling of the HTCMC compared to the plain copper that showed about 24 K of wall superheat at the same heat flux, as shown in Figure 5. In addition, the higher wall superheat jump for the plain surface compared with that of the HTCMC was observed at nucleate boiling incipience. For example, at 20 K subcooling (yellow circle in Figure 5) the temperature jump was ~5 K before boiling incipience, whereas it was about only ~1 K for HTCMC at the same subcooling temperature. This represents the fact that the HTCMC is more effective on nucleate boiling incipience at subcoolings as well [12]. In addition, Figure 5 shows the CHF values of both the HTCMC and the plain surfaces increased as subcooling increased so that the CHF value of the HTCMC was 3,820 kW/m^2 and that of the plain surface was 2,820 kW/m^2 at 30 K subcooling.

Figure 6 shows snapshots obtained with a high speed camera (Phantom, Miro 30) with 2,000 frames per second during boiling experiments with the hovering bubble growth at different subcoolings of the plain surface and the HTCMC at a heat flux of 1,000 kW/m^2. It can be seen that a bubble size of subcooled boiling is smaller at lower bulk liquid temperature because of the condensation of the bubble by the surrounding subcooled liquid. The hovering bubble sizes for both the plain surface and the HTCMC are comparable at the same subcooling since the hovering bubble cycles of both the HTCMC and the plain surface are similar, but they decrease as the degree of subcooling increases due to the condensation of the surrounding subcooled liquid. On the other hand, the bubbles below the large hovering bubble of the HTCMC are much smaller, and the number of bubbles is much higher than that of the plain surface. The NBHT of the HTCMC was significantly enhanced compared to the plain surface at the same heat flux of 1,000 kW/m^2, as the wall superheat of the HTCMC was ~3 K, whereas that of the plain surface was ~20 K. The hovering bubble cycles of both the HTCMC and the plain surface were comparable at the same subcooling, but they decreased as the subcooling increased from ~40 milliseconds (ms) at saturation to ~20 ms at 20 K subcooling. In case of the degree of subcooling at 30 K, no hovering bubbles were observed for both surfaces at 1,000 kW/m^2 because of rapid condensation due to high subcooling. Only mist-like tiny bubbles rose upward, as shown in Figure 6, and the mist-like bubbles appeared to be smaller for the microporous surface boiling.

The maximum hovering bubble sizes near the CHF are observed in Figure 7 and they decrease as the degree of subcooling increases, although the CHF values become higher as the subcooling increases. However, the maximum hovering bubble size of the HTCMC is larger than that of the plain surface because of higher CHF values with the HTCMC surfaces. To summarize, it is observed that the hovering

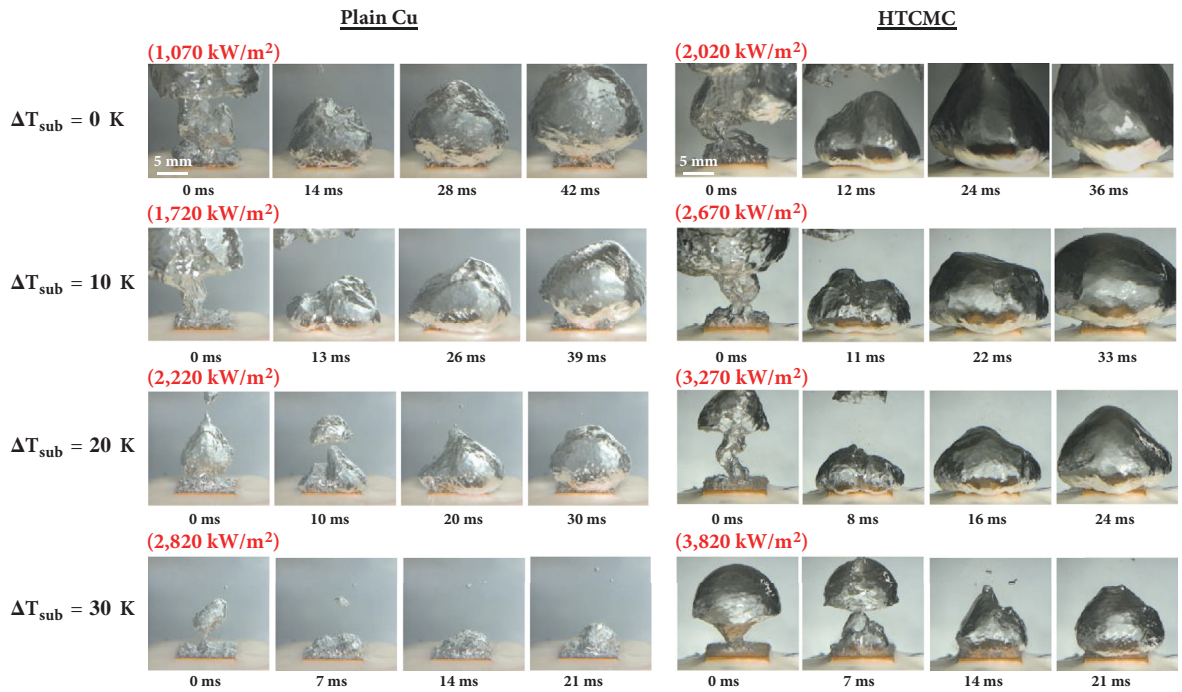

FIGURE 7: Nucleate boiling comparison of Plain Cu and HTCMC with different subcooled temperatures (ΔT_{sub}) of 0 K, 10 K, 20 K, and 30 K at the CHF. The values in parentheses represent applied heat fluxes.

bubble sizes of the HTCMC and he plain surface are similar at the same heat flux as shown in Figure 6, but their size decreases as the subcooling increases and increases as the heat flux increases the vapor bubble generating rate increases as the heat flux increases.

It is well known that CHF increases with subcooling. According to Kutateladze [1], CHF occurs when vapor films are generated between the heater wall and the liquid, so in order to create a vapor film in a subcooled liquid, it is necessary to supply at least enough heat equal to that required for a critical rate of vapor formation in a saturated liquid. This causes CHF enhancement in subcooling. Another explanation for the CHF increase in subcooling is the ease of access for liquid to flow toward a heated surface by condensation of vapor leaving the region of the heated surface through the subcooled pool [17]. The results showed that the CHF of both the plain surface and the HTCMC linearly increases with subcooling and this agrees with previous research [1–3, 5–11, 13, 20, 21], as shown in Figure 8. The increasing rates of CHF due to the subcooling are similar for both the plain and HTCMC surfaces as ~60 kW/m^2 per degree of subcooling. This implies that a similar amount of subcooled water near the heated surfaces is heated to saturation at the same subcooling for both the plain and HTCMC surfaces. As a result, the CHF values of the HTCMC remained ~1,000 kW/m^2 higher than those of the plain surface throughout the subcoolings tested. In case of 30 K of subcooling, the CHF of the plain surface was 2,820 kW/m^2, whereas that of the HTCMC was 3,820 kW/m^2.

The linearity of the CHF with the degree of subcooling was often normalized by the CHF value at saturation [8]:

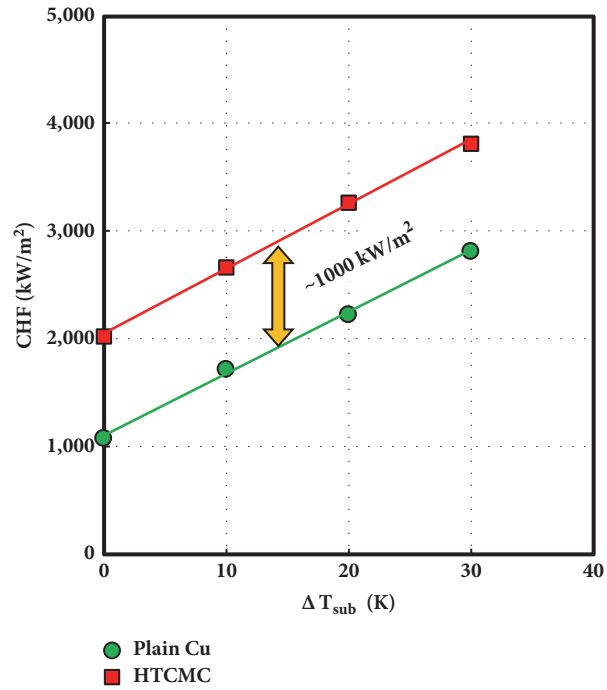

FIGURE 8: CHF comparison of HTCMC and plain surface with subcooling.

$$\frac{q''_{CHF,sub}}{q''_{CHF,sat}} = 1 + C_{sub}\Delta T_{sub} \quad (7)$$

C_{sub} is an empirical constant, and ΔT_{sub} ($=\Delta T_{sat}$-T_l) is the degree of subcooling. The linear increase in normalized CHF

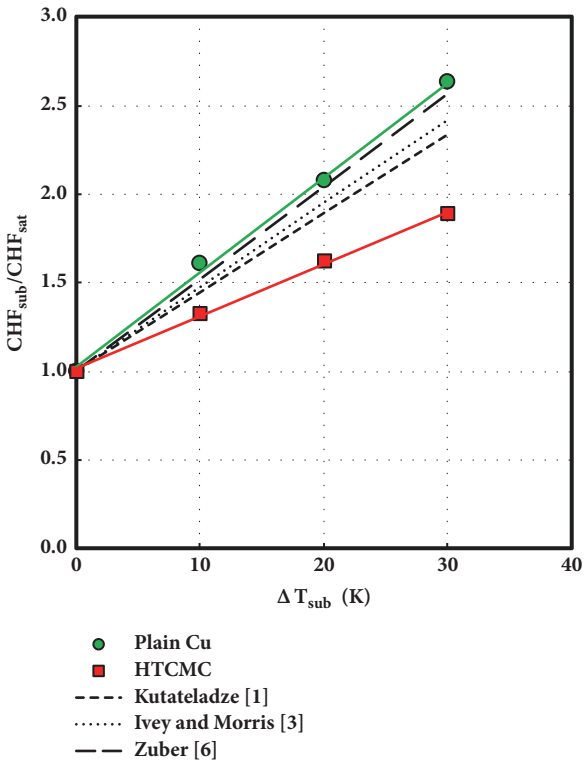

Figure 9: Normalized CHF comparison of HTCMC and plain surface with subcooling.

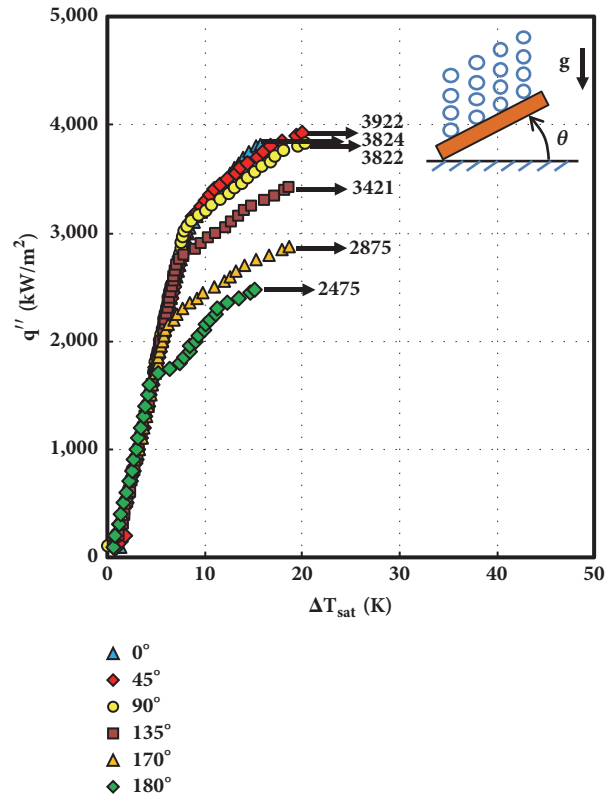

Figure 10: Boiling curves of HTCMC with various orientation angles at 30 K subcooling.

Table 1: The coefficient "C_{sub}" of (5) for subcooled CHF.

Result/Model	C_{sub}
Plain Cu (Present)	0.0535
HTCMC (Present)	0.0296
Kutateladze [1]	0.0446
Ivey and Morris [3]	0.0482
Zuber [6]	0.0522

with the degree of subcooling is plotted in Figure 9 for water. For the plain surface, the current experiment showed the constant C_{sub} value to be 0.0535 (Table 1) by linear curve fitting. This means a 5.3% increase in the CHF per degree of subcooling. The increment of the plain surface in water is higher than dielectric fluids such as of FC-72 (3.1%) [8] or PF-5600 (2.1%) [13] on a plain surface. This shows that water is more efficient cooling fluid than the others for single-phase, and the CHF thus increases efficiently in subcooled boiling heat transfer compared to the other fluids. The current data of the plain surface were compared with some of the existing CHF correlations and best matched with Zuber's correlation, as shown in Table 1 and Figure 9. For the HTCMC case, the coefficient of C_{sub} turned out to be 0.0296. Thus, it implies that the rate of CHF increase based on the CHF at saturation of the HTCMC was smaller due to the higher CHF value at saturation. However, the absolute values of increment in CHF for the HTCMC are similar to those of the plain surface, as mentioned above.

The orientation effects on pool boiling with 30 K of subcooling for the HTCMC were examined in order to investigate the combined effects of orientation and subcooling. The heater orientations were varied from 0° to 180°. The results showed that the boiling curves collapsed with single line heat fluxes up to ~1,700 kW/m^2, as shown in Figure 10. The results are consistent with the orientation effects on pool boiling heater transfer of the HTCMC surface at saturation [22]. This implies that the NBHT is not affected much by heater orientations, neither at saturation nor subcooling. The wall superheat started to increase faster as the heat flux increased to higher values due to different partial dryout situations. The CHF values were 3,800–3,900 kW/m^2 at the inclination angles between 0° and 90° and they did not change much, whereas they decreased down to 2,475 kW/m^2 as the inclination angle increased at the downward facing directions (from 90° to 180°) due to a higher residence time of vapor bubbles on the surface, causing dryout by blocking cold liquid access onto the heater surface.

The deceasing CHF trend for facing down cases is similar to the orientation effect on the boiling at saturation [22] as shown in Figure 11. In addition, the CHF further sharply decreases between 170° and 180°, and this angle is called a transition angle. The value of the transition angle is consistent with previous studies [22–25]. Based on the experimental results of CHF values for orientation at 30 K of subcooling for the HTCMC surface, the orientation effect can be classified into three regions: upward to vertical (0–90°) where the

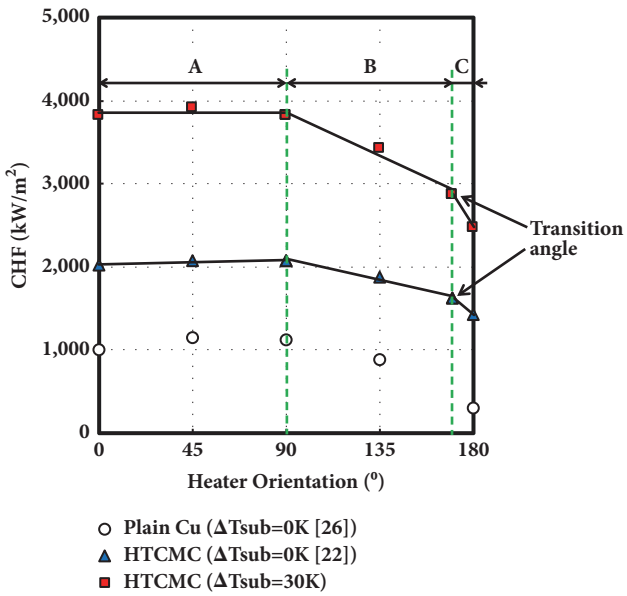

Figure 11: CHF comparison of HTCMC with orientation between saturation and 30 K subcooling; A: upward to vertical (0–90°), and B: vertical to downward facing (90–170°), and C: downward facing to complete downward (170–180°).

CHF maintains close values; vertical to inclined downward facing (90–170°) where the CHF linearly decreases with the orientation angle; and further downward facing (170–180°) where the CHF abruptly decreases just as Jun et al. [22] observed in the heater orientation effects at saturation for the HTCMC. It should be also noted in Figure 11 that the decrease in the CHF at 170–180° was much less for the HTCMC cases compared to the drastic decrease of CHF for the plain Cu case observed in Kwark et al. [26]. Delaying the dryout and the CHF of the heated surface when it is downward facing is highly beneficial factor of using HTCMC surfaces.

4. Conclusions

The subcooling effects of pool boiling heat transfer were studied experimentally at subcoolings of 10, 20, and 30 K for a Cu-HTCMC and a plain surface, and the boiling heat transfer and the CHF were compared. The results showed that the nucleate boiling heat transfer did not change much with the degree of subcooling for both the HTCMC and the plain surface. However, the CHF linearly increased with the similar rates of 60 kW/m^2 per degree for both surfaces, so the CHF values of the HTCMC stayed about ~1,000 kW/m^2 higher than those of the plain surface throughout the subcooling. For the plain surface, the CHF values were well matched with Zuber's correlation for subcooling. The combined effect of orientation and subcooling was also investigated for the HTCMC at 30 K subcooling and it was compared with the data at saturation. The results showed that the nucleate boiling heat transfer was close up to ~1,700 kW/m^2 regardless of the heater orientation. The CHF values of the HTCMC at different orientations with the subcooling 30 K showed the same trend with those of saturation case. The CHF values for Cu-HTCMC stayed at 3,800~3,900 kW/m^2 at upward to vertical orientation (0–90°) and linearly decreased at downward facing orientations (90–170°) and then sharply decreased at further downward facing angles (170–180°) to ~2,500 kW/m^2.

Nomenclature

C: Empirical constant
c_p: Specific heat [J/kgK]
g: Gravitational acceleration [m/s^2]
h: Boiling heat transfer coefficient [W/m^{2}K]
k: Thermal conductivity [W/mK]
L: Latent heat of vaporization [J/kg]
R: Radius [m]
q'': Heat flux [W/m^2]
T: Temperature [K]
ΔT_{sat}: Wall superheat [K]
ΔT_{sub}: Degree of subcooling [K]
V: Volume [m^3]
v: Specific volume [m^3/kg].

Greek Symbols

α: Thermal diffusivity [m^2/s]
σ: Surface tension [N/m]
ε: Porosity
τ: Bubble residence time [s].

Subscripts

c: Cavity
cp: Copper powder
l: Liquid
lv: Liquid-vapor
m: Microporous coating
p: Plain
sat: Saturated conditions
sub: Subcooled conditions
t: Total.

Data Availability

The data used to support the findings of this study are available from the corresponding author upon request.

Disclosure

Partial work of this study was presented at Second Thermal and Fluids Engineering Conference, 2017.

Conflicts of Interest

The authors declare that they have no conflicts of interest.

Acknowledgments

This work was supported by the National Research Foundation of Korea (NRF) grant funded by the Korean government (Ministry of Science and ICT; Grant no. 2017 M2A8A4015274).

References

[1] S. S. Kutateladze, "Heat Transfer in Condensation and Boiling," Tech. Rep., State Scientific and Technical Publishers of Literature on Machinery, 1952.

[2] S. Kutateladze and L. Schneiderman, "Experimental study of influence of temperature of liquid on change in the rate of boiling," USAEC Report AECtr. 3405, 1953.

[3] H. Ivey and D. Morris, *On the Relevance of the Vapour-Liquid Exchange Mechanism for Sub-Cooled Boiling Heat Transfer at High Pressure*, Reactor Development Division, Atomic Energy Establishment, 1962.

[4] K. Engelburg-Forster and R. Grief, "Heat transfer to a boiling liquid-mechanism and correlations," *Journal of Heat Transfer*, vol. 81, pp. 43–53, 1959.

[5] H. Ivey and D. Morris, "Critical heat flux of saturation and subcooled pool boiling in water at atmospheric pressure," in *Proceedings of the 3rd International Heat Transfer Conference*, vol. 4, pp. 129–142, 1966.

[6] N. Zuber, M. Tribus, and J. W. Westwater, "The hydrodynamic crisis in pool boiling of saturated and subcooled liquids," *International Developments in Heat Transfer*, vol. 27, pp. 220–236, 1963.

[7] U. Hwang and K. Moran, "Boiling heat transfer of silicon integrated circuits chip mounted on a substrate," in *Proceedings of the Winter Annual Meeting*, vol. 1, pp. 53–59, 1981, Boiling heat transfer of silicon integrated circuits chip mounted on a substrate, 1.

[8] I. Mudawar and T. M. Anderson, "Parametric investigation into the effects of pressure, subcooling, surface augmentation and choice of coolant on pool boiling in the design of cooling systems for high-power-density electronic chips," *Journal of Electronic Packaging, Transactions of the ASME*, vol. 112, no. 4, pp. 375–382, 1990.

[9] A. A. Watwe, A. Bar-Cohen, and A. McNeil, "Combined pressure and subcooling effects on pool boiling from a PPGA chip package," *Journal of Electronic Packaging, Transactions of the ASME*, vol. 119, no. 2, pp. 95–105, 1997.

[10] K. N. Rainey, S. M. You, and S. Lee, "Effect of pressure, subcooling, and dissolved gas on pool boiling heat transfer from microporous surfaces in FC-72," *Journal of Heat Transfer*, vol. 125, no. 1, pp. 75–83, 2003.

[11] K. N. Rainey, S. M. You, and S. Lee, "Effect of pressure, subcooling, and dissolved gas on pool boiling heat transfer from microporous, square pin-finned surfaces in FC-72," *International Journal of Heat and Mass Transfer*, vol. 46, no. 1, pp. 23–35, 2003.

[12] J. L. Parker and M. S. El-Genk, "Enhanced saturation and subcooled boiling of FC-72 dielectric liquid," *International Journal of Heat and Mass Transfer*, vol. 48, no. 18, pp. 3736–3752, 2005.

[13] M. S. El-Genk and A. Suszko, "Effects of inclination angle and liquid subcooling on nucleate boiling on dimpled copper surfaces," *International Journal of Heat and Mass Transfer*, vol. 95, pp. 650–661, 2016.

[14] S. J. Kline and F. McClintock, "Describing uncertainties in single-sample experiments," *Mechanical Engineering*, vol. 75, pp. 3–8, 1953.

[15] S. Jun, J. Kim, D. Son, H. Y. Kim, and S. M. You, "Enhancement of Pool Boiling Heat Transfer in Water Using Sintered Copper Microporous Coatings," *Nuclear Engineering and Technology*, vol. 48, no. 4, pp. 932–940, 2016.

[16] S. Jun, H. Wi, A. Gurung, M. Amaya, and S. M. You, "Pool boiling heat transfer enhancement of water using brazed copper microporous coatings," *Journal of Heat Transfer*, vol. 138, no. 7, Article ID 071502, 2016.

[17] V. P. Carey, *Liquid-Vapor Phase-Change Phenomena*, Taylor & Francis Group, New York, NY, USA, 2nd edition, 2008.

[18] E. E. Anderson, *Thermodynamics*, PWS Publishing Company, Boston, Mass, USA, 1st edition, 1994.

[19] A. Ono and H. Sakashita, "Liquid-vapor structure near heating surface at high heat flux in subcooled pool boiling," *International Journal of Heat and Mass Transfer*, vol. 50, no. 17-18, pp. 3481–3489, 2007.

[20] M. S. El-Genk and A. Suszko, "Saturation and subcooled CHF correlations for PF-5060 dielectric liquid on inclined rough copper surfaces," *Multiphase Science and Technology*, vol. 26, no. 2, pp. 139–170, 2014.

[21] T. Inoue, N. Kawae, and M. Monde, "Effect of subcooling on critical heat flux during pool boiling on a horizontal heated wire," *Heat and Mass Transfer*, vol. 33, no. 5-6, pp. 481–488, 1998.

[22] S. Jun, J. Kim, S. M. You, and H. Y. Kim, "Effect of heater orientation on pool boiling heat transfer from sintered copper microporous coating in saturated water," *International Journal of Heat and Mass Transfer*, vol. 103, pp. 277–284, 2016.

[23] Y. H. Kim and K. Y. Suh, "One-dimensional critical heat flux concerning surface orientation and gap size effects," *Nuclear Engineering and Design*, vol. 226, pp. 277–292, 2003.

[24] S. H. Yang, W.-P. Baek, and S. H. Chang, "Pool-boiling critical heat flux of water on small plates: Effects of surface orientation and size," *International Communications in Heat and Mass Transfer*, vol. 24, no. 8, pp. 1093–1102, 1997.

[25] A. H. Howard and I. Mudawar, "Orientation effects on pool boiling critical heat flux (CHF) and modeling of CHF for near-vertical surfaces," *International Journal of Heat and Mass Transfer*, vol. 42, no. 9, pp. 1665–1688, 1999.

[26] S. M. Kwark, M. Amaya, R. Kumar, G. Moreno, and S. M. You, "Effects of pressure, orientation, and heater size on pool boiling of water with nanocoated heaters," *International Journal of Heat and Mass Transfer*, vol. 53, no. 23-24, pp. 5199–5208, 2010.